Opportunistic Model Intercomparison of Miocene Ocean Circulation – MioMIP1

Trusha J. Naik[1,2], A. M. de Boer[1,2], H. K. Coxall[1,2], N. J. Burls[3], C. D. Bradshaw[4,5], Y. Donnadieu[6], A. Farnsworth[7,8], A. Frigola[9,10], N. Herold[11], M. Huber[12], M. P. Karami[13], G. Knorr[14], A. N. LeGrande[15,16], Y. Li[7], G. Lohmann[10,14], D. J. Lunt[7], M. Prange[10], Y. Zhang[17]

Bolin Centre for Climate Research | Stockholm University

Email: trusha.naik@geo.su.se

Why study Miocene ocean circulation?

- Miocene (~23-5 Ma) is a warm epoch of the Neogene Period.
- The planet's current ocean circulation pattern, with deep-water formation (DWF) in the North Atlantic and no DWF in the North Pacific, might have evolved sometime during the Miocene (Cramer et al., 2009; McKinley et al., 2019).
- Proxy data suggest reduced DWF in Northern Hemisphere before Miocene (Müller-Michaelis & Uenzelmann-Neben, 2014).
- A number of oceanic gateways were shoaling or deepening during this epoch.
- This study offers a comprehensive examination of factors affecting ocean circulation during the early and middle Miocene (~20-11 Ma) by conducting an opportunistic intercomparison of 14 fully coupled climate model simulations.

Simulations

Model	CO_2 (ppm)	Palaeogeography	Ice Sheets	Target Time Period
CCSM4	400	Herold, Huber and Müller (2011) (updated)	GIS - 0.29e6 km3, AIS - 6.5e6 km3	20-14 Ma
COSMOS	450	Herold, Huber and Müller (2011)+NA/Arctic reconstruction (Ehlers and Jokat, 2013)	No GIS, AIS - Herold et al. (2008)	20-14 Ma
IPSLCM5	560	Poblete et al. (2021), Tethys closed	AIS, no GIS	20 Ma
IPSLCM5_T		Tethys - 120 m		
CCSM3_H	355	Herold, Huber and Müller (2011)	Herold et al. (2008); AIS height reduced by 1000 m	20-14 Ma
CCSM3_F	400	Frigola et al. (2018)	No GIS, AIS - 6e6 km3	16.7-14.5 Ma
HadCM3L_F1	400	Getech Plc.	AIS, No GIS	15.9-13.8 Ma
HadCM3L_F2	760			15.9-13.8 Ma
HadCM3L_F3	400			13.8-11.6 Ma
HadCM3L_L1	494	Scotese and Wright (2018)		15.9-13.8 Ma
HadCM3L_B1	400	Marwick (2007)	No GIS, No AIS	15.9-11.6 Ma
HadCM3L_B2	400		No GIS, AIS - 55m SLE	
CESM1	400	Herold, Huber and Müller (2011) (updated)	GIS - 0.29e6 km3, AIS - 6.5e6 km3	20-14 Ma
GISS	456	Frigola et al. (2018)	No GIS, AIS - 6e6 km3	16.7-14.5 Ma

Affiliations: [1]Department of Geological Sciences, Stockholm University, [2]Bolin Centre for Climate Research, Sweden, [3]Department of Atmospheric, Oceanic and Earth Sciences, Center for Ocean-Land Atmosphere Studies, George Mason University, USA, [4]The Global Systems Institute, University of Exeter, UK, [5]Met Office Hadley Centre, UK, [6]Aix Marseille University, CNRS, IRD, Coll France, INRA, CEREGE, France, [7]School of Geographical Sciences, University of Bristol, UK, [8]Tibetan Plateau Earth System, Environment and Resources (TPESER), Institute of Tibetan Plateau Research, Chinese Academy of Sciences, China, [9]Barcelona Supercomputing Center, Spain, [10]MARUM – Center for Marine Environmental Sciences, University of Bremen, Germany, [11]School of Life and Environmental Sciences, The University of Sydney, Australia, [12]Department of Earth, Atmospheric, and Planetary Sciences, Purdue University, USA, [13]Rossby Centre, Swedish Meteorological and Hydrological Institute, Sweden, [14]Alfred Wegener Institute Helmholtz Centre for Polar and Marine Research, Germany, [15]NASA Goddard Institute for Space Studies, USA, [16]Center for Climate Systems Research, Columbia University, USA, [17]State Key Laboratory of Marine Environmental Science, College of Ocean & Earth Sciences, Xiamen University, China.

Evolution of oceanic gateways during Miocene

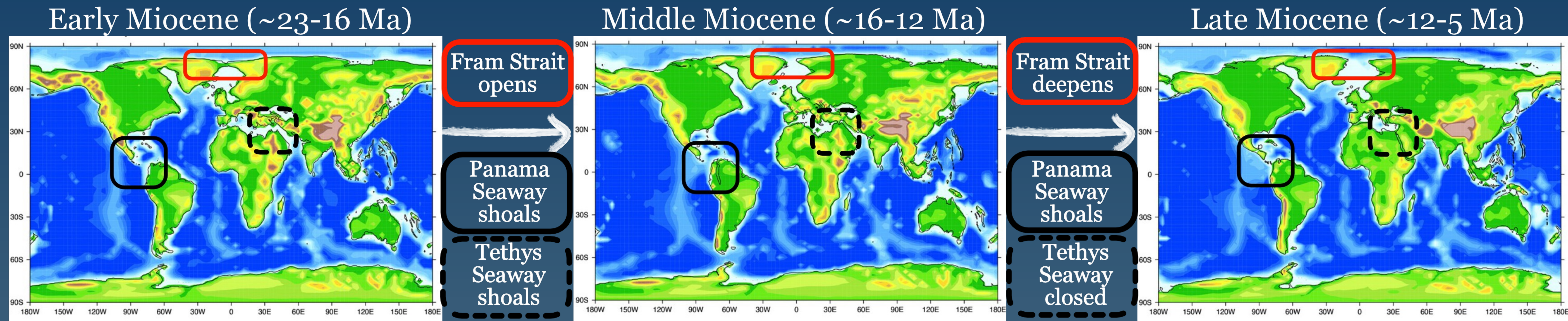

Fig. 1: The evolution of some major gateways throughout the Miocene is shown here. The red box indicates the Fram Strait, the black dashed box indicates the Tethys Seaway and the black solid box indicates the Panama Seaway. The shoaling/deepening of these oceanic gateways altered the pathways for exchange of water masses between oceanic basins and thus likely affected the large scale ocean circulation. (Modified from Steinthorsdottir et al., 2021)

Results

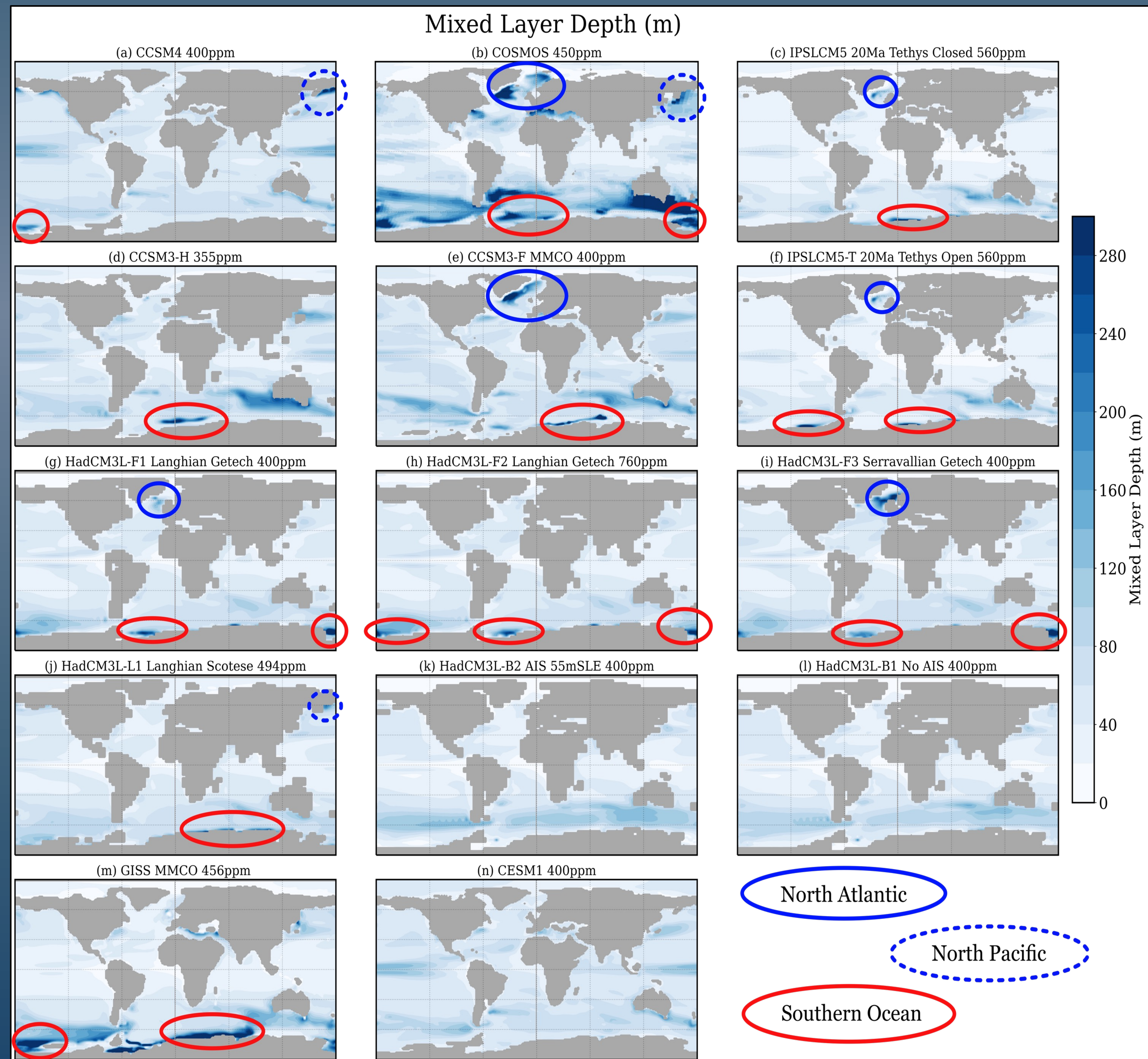

Fig. 2: The annual average mixed layer depth (MLD). Dark blue areas in polar and subpolar seas signify potential deepwater formation regions. Most simulations exhibit deep MLDs in the Southern Ocean. In the Northern Hemisphere, 6 simulations show deep MLDs in the North Atlantic, while 3 show deep MLDs in the North Pacific Ocean. A deep MLD cut-off of 300 m is utilized, due to the availability of only annual average values for all simulations, which offers the best spatial distribution of persistent polar sinking regions. Table 1 specifies the overturning strength in each basin. AIS= Antarctic Ice Sheet, MMCO – Miocene Climatic Optimum

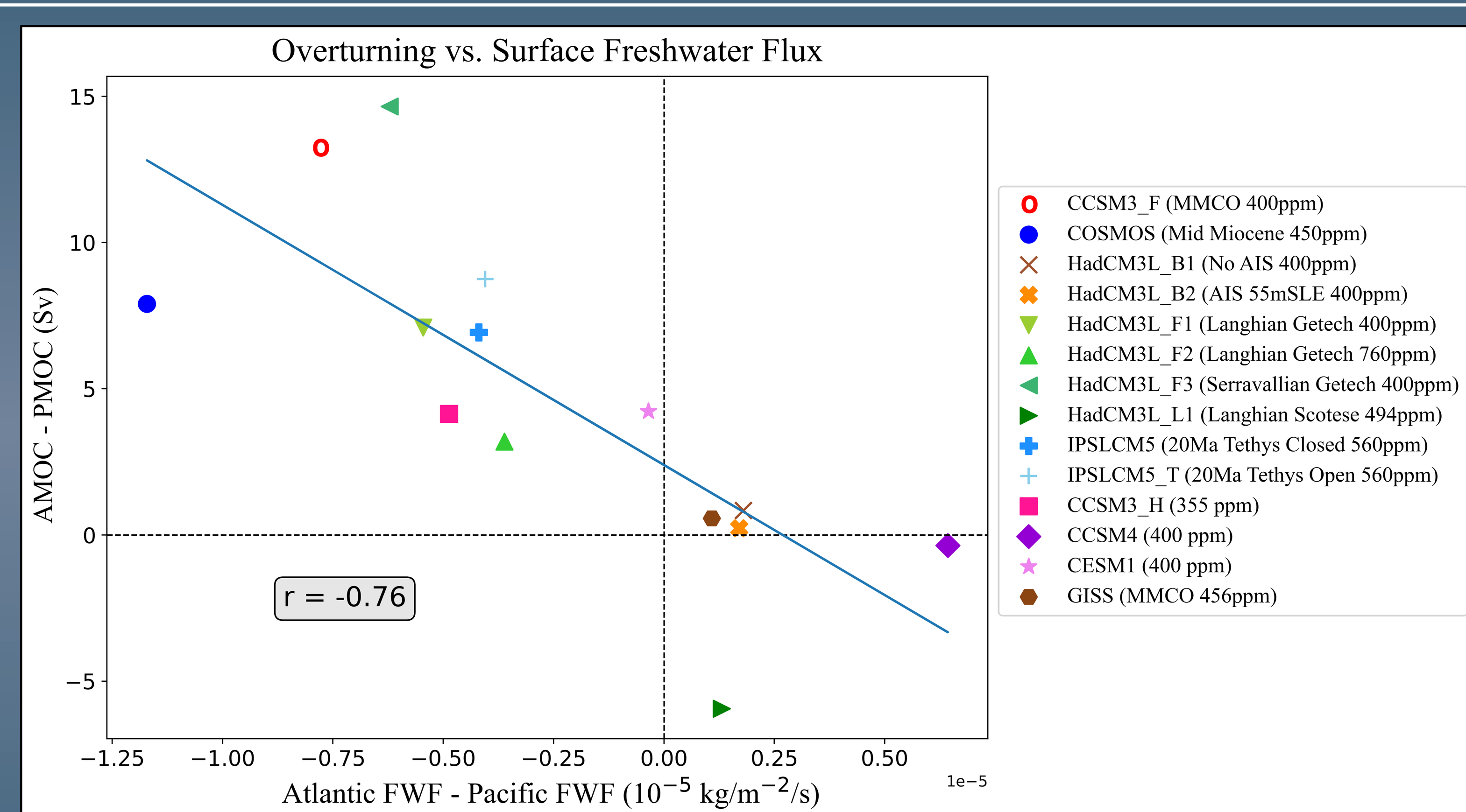

Fig. 3: Dependence of difference between AMOC and PMOC strength on the difference in surface freshwater flux (FWF) received by North Atlantic and North Pacific. The surface freshwater flux is calculated as Precipitation - Evaporation + Runoff. The annotated box with r=0.76 is the Pearson correlation coefficient between FWF and overturning. 1 Sv = 10^6 m^3/s. AIS= Antarctic Ice Sheet, MMCO – Miocene Climatic Optimum

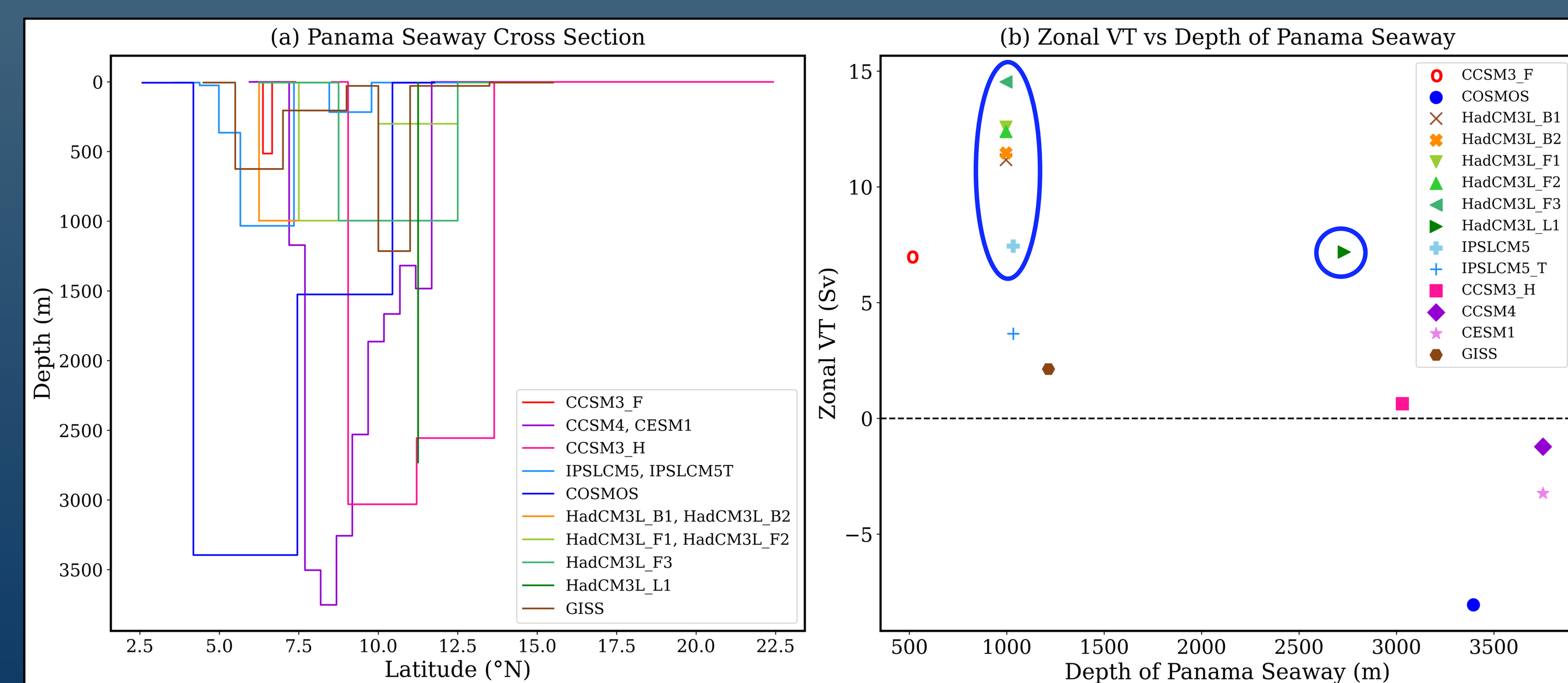

Fig. 4: The cross section of the Panama Seaway (Fig. 4a) and the dependence of zonal volume transport (VT) through the Panama Seaway on the depth of the gateway (Fig. 4b) is shown. The simulations circled in blue in Fig. 4b are the simulations with a closed Tethys Seaway. Positive values in Fig. 4b indicate the net zonal VT is eastward or into the Atlantic and negative values indicate the VT is into the Pacific.

References: **Cramer et al. (2009)**. Paleoceanography, 24(4). **Frigola et al. (2018).** Geoscientific Model Development, 11(4), 1607-1626. **Herold et al. (2008).** Geochemistry, Geophysics, Geosystems, 9(10). **Herold et al. (2011).** Journal of climate, 24(24), 6353-6372. **Marwick (2007).** The Micropalaeontological Society Special Publications, Geological Society of London. **McKinley et al. (2019)**. Earth and Planetary Science Letters, 521, 139-149. **Müller-Michaelis & Uenzelmann-Neben (2014).** Deep Sea Research Part I: Oceanographic Research Papers, 93, 21-34. **Poblete et al. (2021).** Earth-Science Reviews, 214, 103508. **Scotese & Wright (2018)**. Paleomap Proj. **Steinthorsdottir et al. (2021).** Paleoceanography and Paleoclimatology, 36(4). **Thomas et al. (2014)**. Paleoceanography, 29(5), 454-469.

Table 1: The strength of the overturning in each basin is given in this table. AMOC - Atlantic Meridional Overturning Circulation, PMOC – Pacific Meridional Overturning Circulation, SOMOC – Southern Ocean Meridional Overturning Circulation.

Model	AMOC Strength (Sv)	PMOC Strength (Sv)	SOMOC Strength (Sv)
CCSM4	6.55	6.91	-13.00
COSMOS	13.11	5.21	-3.30
IPSLCM5	6.99	0.06	-16.60
CCSM3-H	5.55	1.41	-17.80
CCSM3-F	14.21	0.97	-27.90
IPSLCM5-T	8.79	0.04	-14.60
HadCM3L-F1	8.11	1.02	-17.50
HadCM3L-F2	4.26	1.07	-18.70
HadCM3L-F3	15.67	1.02	-19.70
HadCM3L-L1	3.68	9.62	-23.10
HadCM3L-B2	1.25	1.02	-13.00
HadCM3L-B1	1.94	1.10	-11.10
GISS	2.26	1.69	-26.71
CESM1	4.90	0.67	-6.00

Conclusions

- Southern Ocean is the dominant basin of deep overturning in most of the simulations (Table 1), in agreement with proxy records (Thomas et al., 2014).
- Weak but consistent AMOC present in majority of simulations, PMOC present in 3 simulations (Table 1, Fig. 2).
- Surface freshwater flux controls the dominant overturning basin across the simulations in the Northern Hemisphere (Fig. 3).
- Arctic Ocean was substantially fresher than modern during the Miocene.
- The flow through the Panama Seaway is affected by the Tethys Seaway. With an open Tethys, as the Panama Seaway shoals, the VT turns from westward to eastward (Fig. 4).
- Flow through Panama Seaway is eastward always when Tethys Seaway is closed.

Next Steps

- Investigate the depth structure of the volume transport through the Panama Seaway further.
- Investigate the effect of orography on the basin with overturning in the Northern Hemisphere.
- Compare the Miocene simulations to the pre-industrial control simulations.

Acknowledgements: I would like to thank the **Albert and Maria Bergström Foundation** and the **Bolin Centre Climate Research School** for granting me funding to cover all expenses for attending the EGU General Assembly 2024.

AMOC:

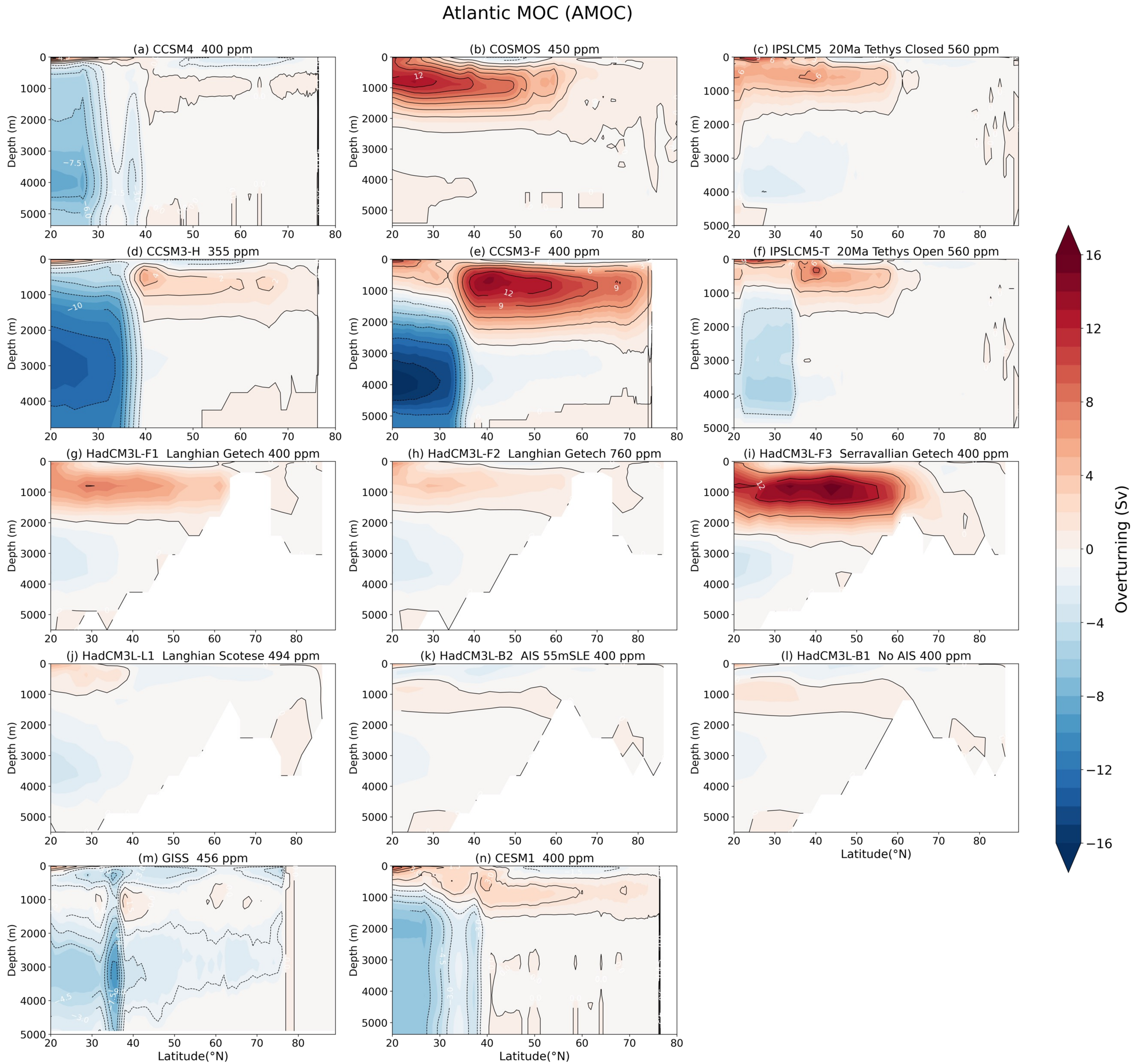
Atlantic MOC (AMOC)
(a) CCSM4 400 ppm
(b) COSMOS 450 ppm
(c) IPSLCM5 20Ma Tethys Closed 560 ppm
(d) CCSM3-H 355 ppm
(e) CCSM3-F 400 ppm
(f) IPSLCM5-T 20Ma Tethys Open 560 ppm
(g) HadCM3L-F1 Langhian Getech 400 ppm
(h) HadCM3L-F2 Langhian Getech 760 ppm
(i) HadCM3L-F3 Serravallian Getech 400 ppm
(j) HadCM3L-L1 Langhian Scotese 494 ppm
(k) HadCM3L-B2 AIS 55mSLE 400 ppm
(l) HadCM3L-B1 No AIS 400 ppm
(m) GISS 456 ppm
(n) CESM1 400 ppm
Depth (m)
Latitude(°N)
Overturning (Sv)

PMOC:

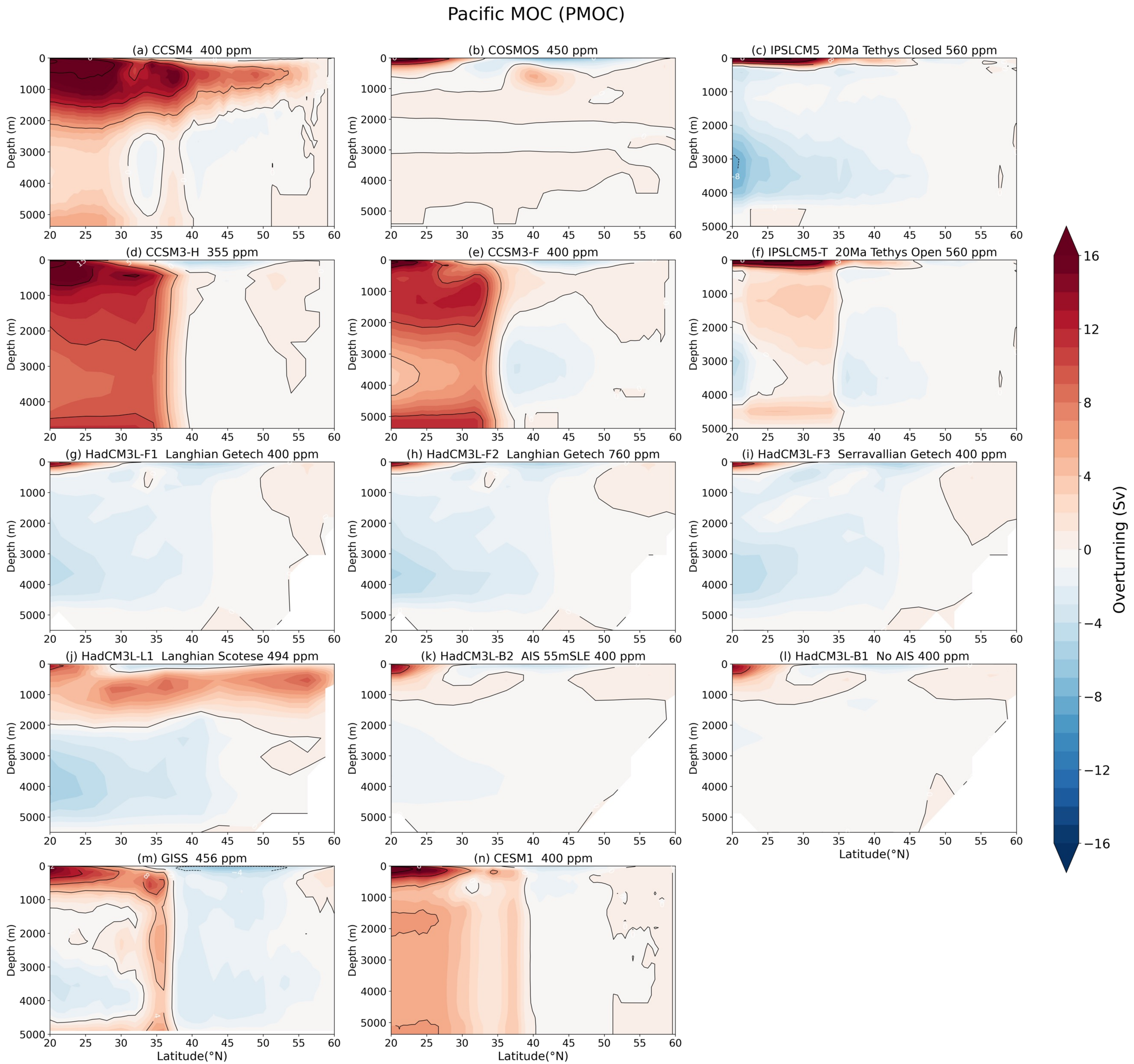
Pacific MOC (PMOC)
(a) CCSM4 400 ppm
(b) COSMOS 450 ppm
(c) IPSLCM5 20Ma Tethys Closed 560 ppm
(d) CCSM3-H 355 ppm
(e) CCSM3-F 400 ppm
(f) IPSLCM5-T 20Ma Tethys Open 560 ppm
(g) HadCM3L-F1 Langhian Getech 400 ppm
(h) HadCM3L-F2 Langhian Getech 760 ppm
(i) HadCM3L-F3 Serravallian Getech 400 ppm
(j) HadCM3L-L1 Langhian Scotese 494 ppm
(k) HadCM3L-B2 AIS 55mSLE 400 ppm
(l) HadCM3L-B1 No AIS 400 ppm
(m) GISS 456 ppm
(n) CESM1 400 ppm
Depth (m)
Latitude(°N)
Overturning (Sv)

GMOC:

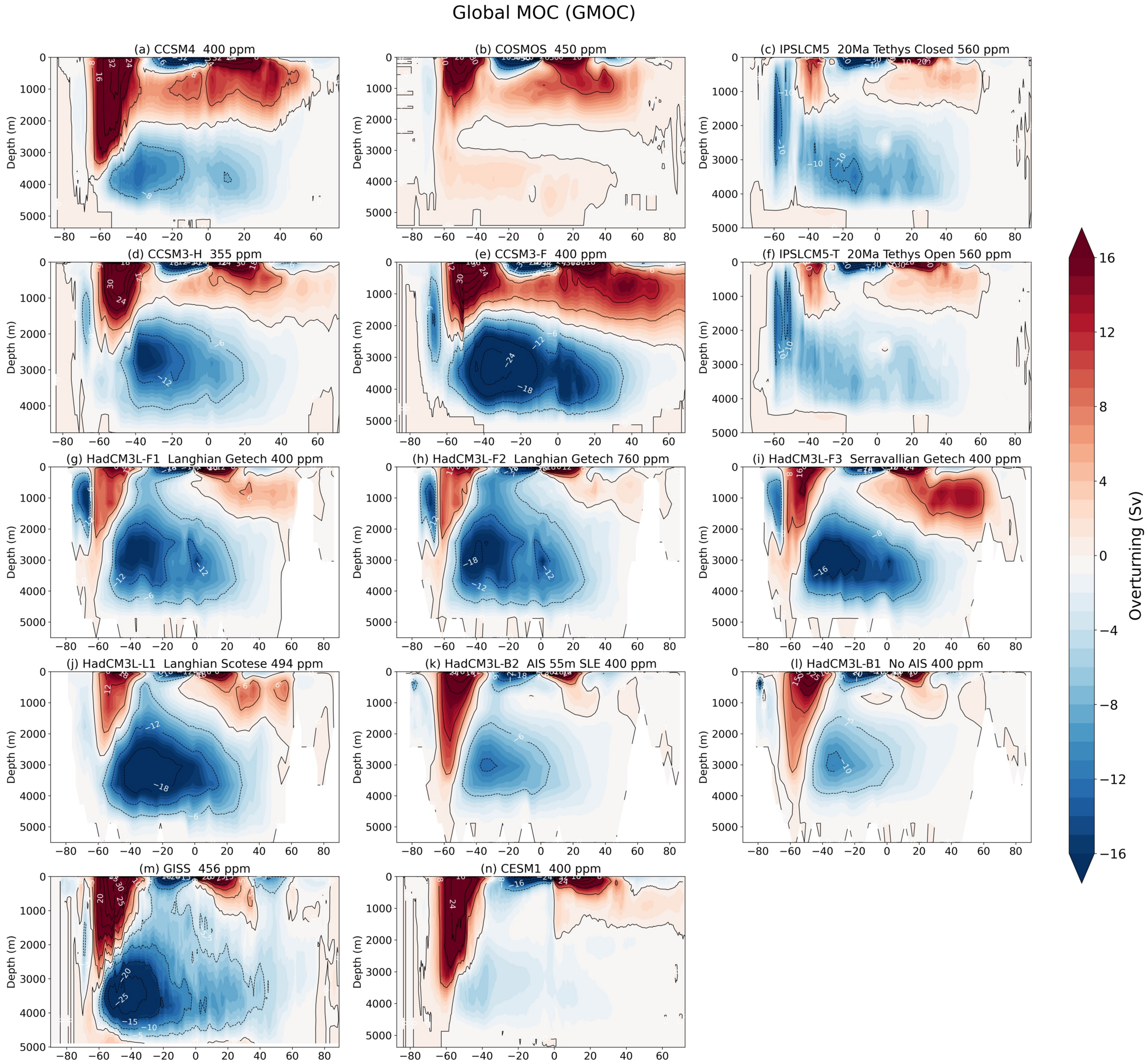
Global MOC (GMOC)
(a) CCSM4 400 ppm
(b) COSMOS 450 ppm
(c) IPSLCM5 20Ma Tethys Closed 560 ppm
(d) CCSM3-H 355 ppm
(e) CCSM3-F 400 ppm
(f) IPSLCM5-T 20Ma Tethys Open 560 ppm
(g) HadCM3L-F1 Langhian Getech 400 ppm
(h) HadCM3L-F2 Langhian Getech 760 ppm
(i) HadCM3L-F3 Serravallian Getech 400 ppm
(j) HadCM3L-L1 Langhian Scotese 494 ppm
(k) HadCM3L-B2 AIS 55m SLE 400 ppm
(l) HadCM3L-B1 No AIS 400 ppm
(m) GISS 456 ppm
(n) CESM1 400 ppm
Depth (m)
Overturning (Sv)
16
12
8
4
0
−4
−8
−12
−16

Salinity vs. Overturning:

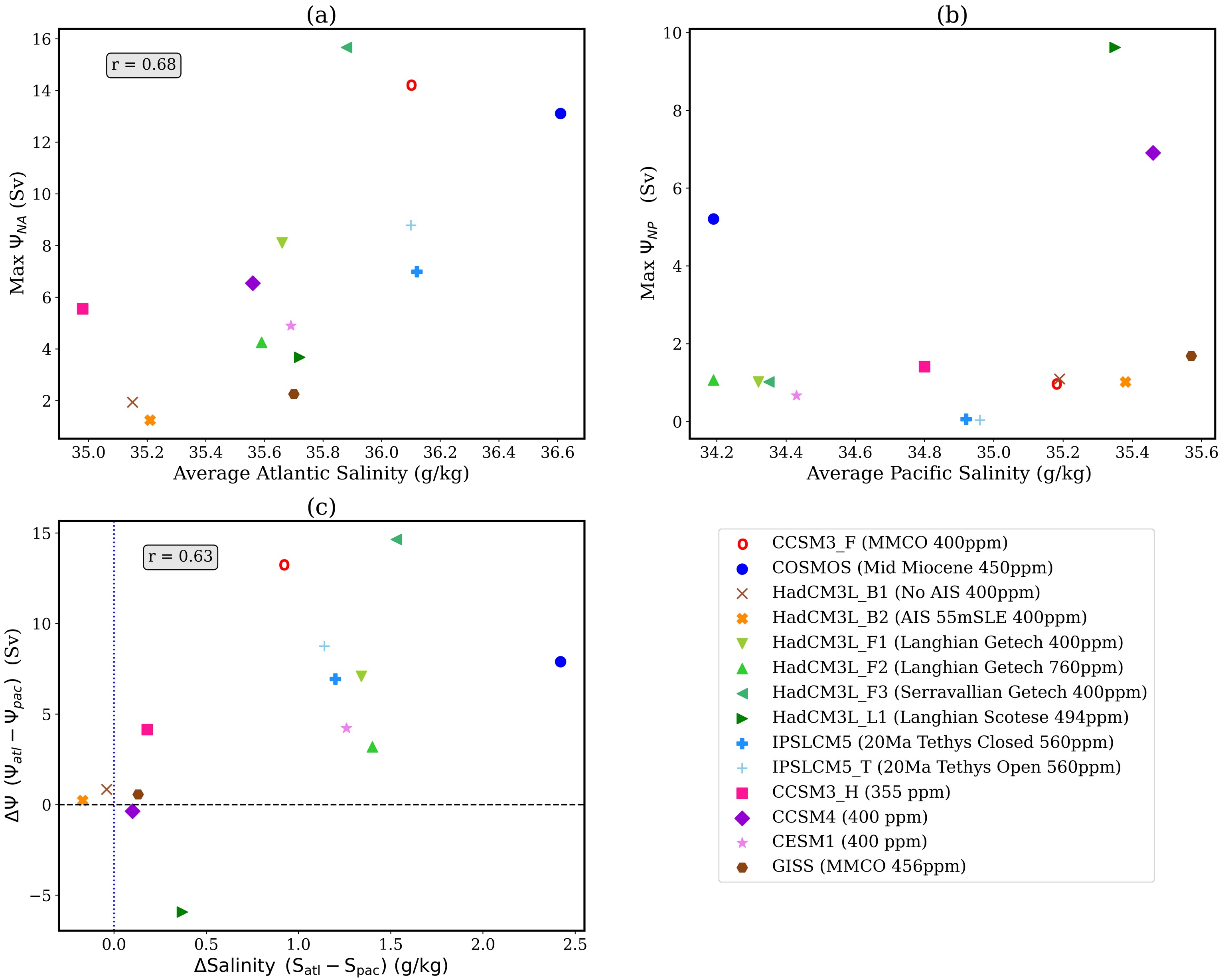

The figure shows the relationship between salinity and the overturning strength. Max ψ_{NA}, ψ_{Atl} – Strength of AMOC
Max ψ_{NP}, ψ_{Pac} – Strength of PMOC.

Tethys Seaway:

Drake Passage:

Fram Strait:

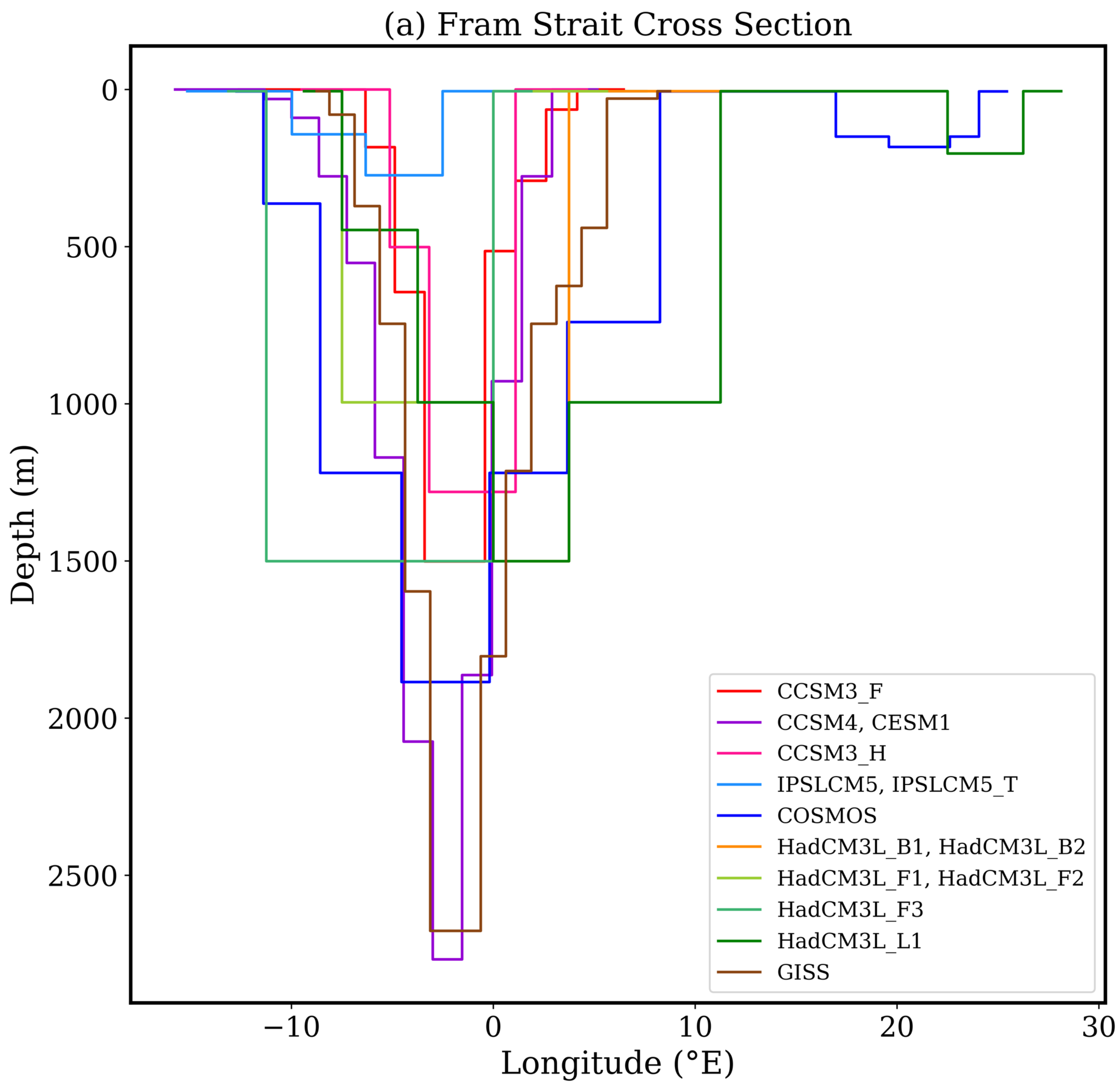
(a) Fram Strait Cross Section
Depth (m)
Longitude (°E)
0
500
1000
1500
2000
2500
−10
0
10
20
30
CCSM3_F
CCSM4, CESM1
CCSM3_H
IPSLCM5, IPSLCM5_T
COSMOS
HadCM3L_B1, HadCM3L_B2
HadCM3L_F1, HadCM3L_F2
HadCM3L_F3
HadCM3L_L1
GISS

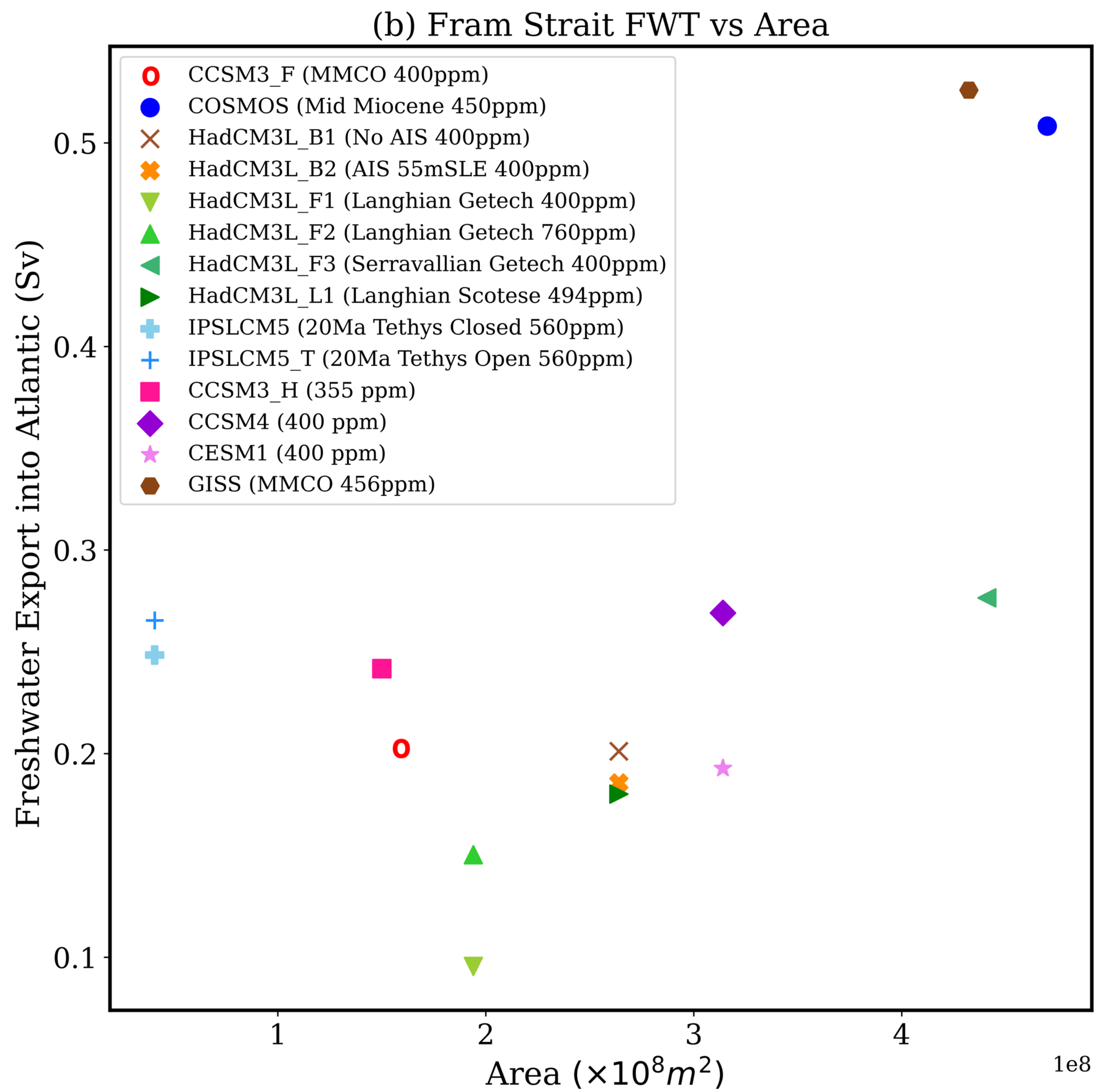
(b) Fram Strait FWT vs Area
Freshwater Export into Atlantic (Sv)
Area ($\times 10^8 m^2$)
1e8
0.1
0.2
0.3
0.4
0.5
1
2
3
4
CCSM3_F (MMCO 400ppm)
COSMOS (Mid Miocene 450ppm)
HadCM3L_B1 (No AIS 400ppm)
HadCM3L_B2 (AIS 55mSLE 400ppm)
HadCM3L_F1 (Langhian Getech 400ppm)
HadCM3L_F2 (Langhian Getech 760ppm)
HadCM3L_F3 (Serravallian Getech 400ppm)
HadCM3L_L1 (Langhian Scotese 494ppm)
IPSLCM5 (20Ma Tethys Closed 560ppm)
IPSLCM5_T (20Ma Tethys Open 560ppm)
CCSM3_H (355 ppm)
CCSM4 (400 ppm)
CESM1 (400 ppm)
GISS (MMCO 456ppm)

Surface Freshwater Flux:

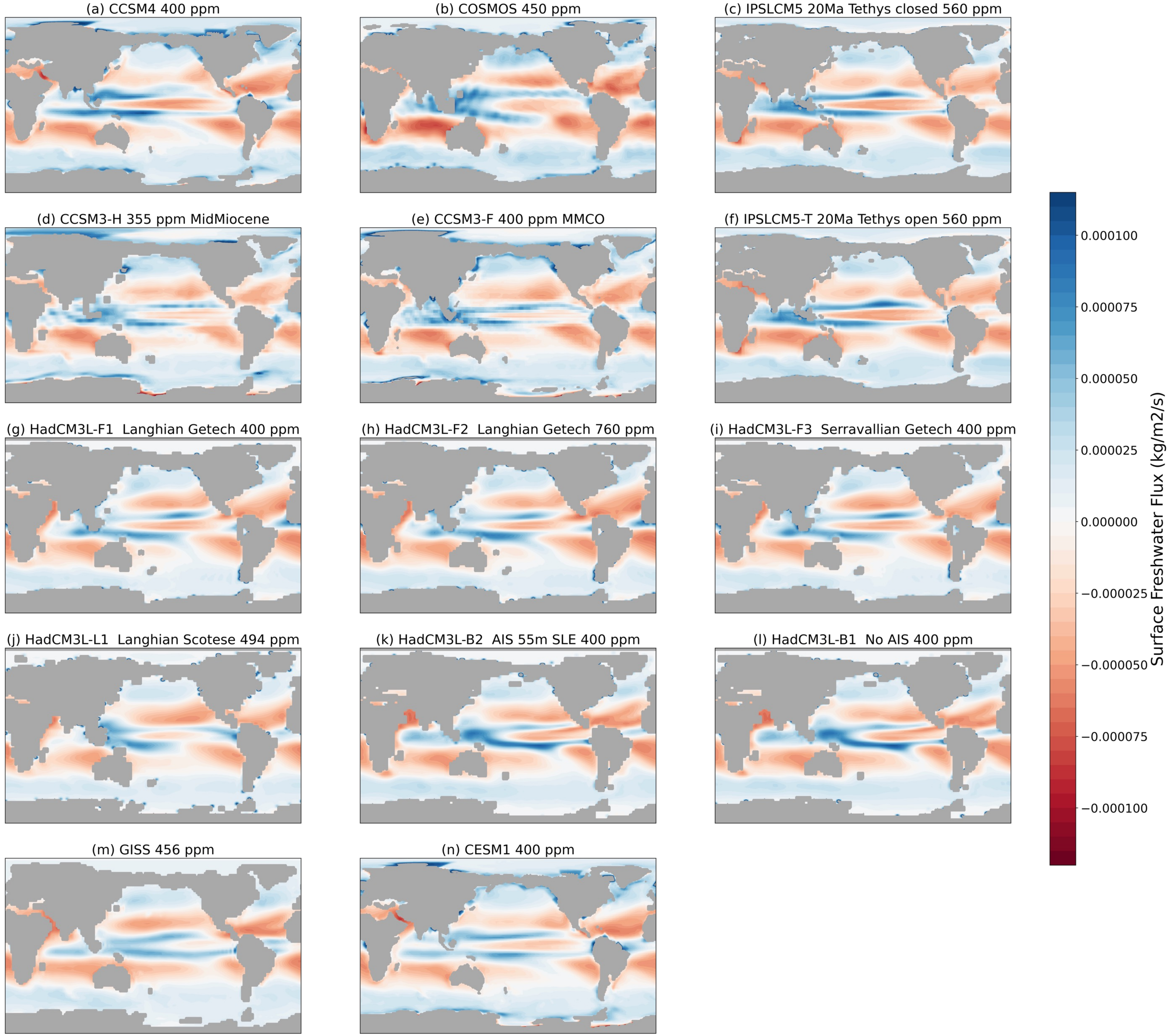

Salinity:

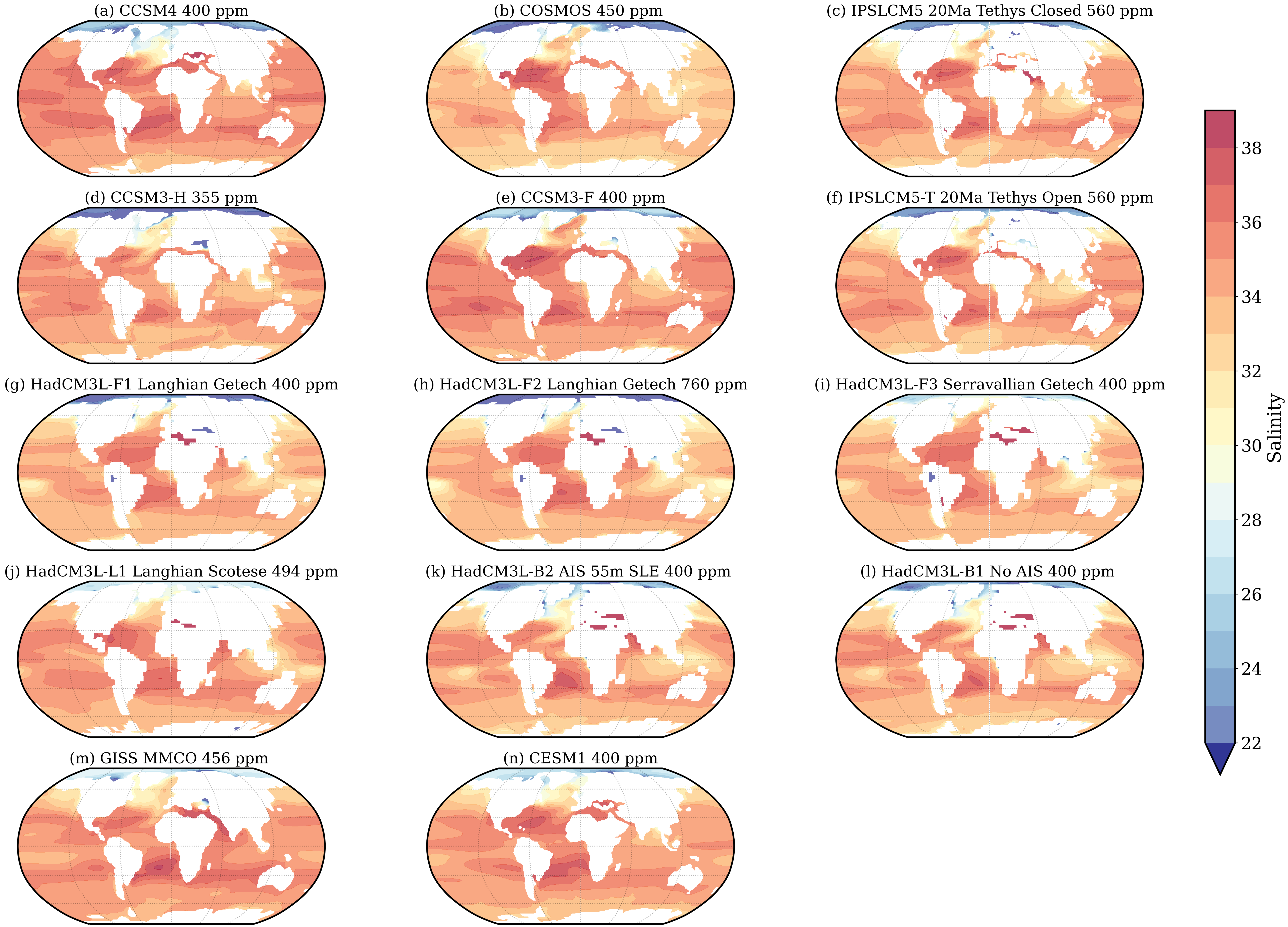

(a) CCSM4 400 ppm
(b) COSMOS 450 ppm
(c) IPSLCM5 20Ma Tethys Closed 560 ppm
(d) CCSM3-H 355 ppm
(e) CCSM3-F 400 ppm
(f) IPSLCM5-T 20Ma Tethys Open 560 ppm
(g) HadCM3L-F1 Langhian Getech 400 ppm
(h) HadCM3L-F2 Langhian Getech 760 ppm
(i) HadCM3L-F3 Serravallian Getech 400 ppm
(j) HadCM3L-L1 Langhian Scotese 494 ppm
(k) HadCM3L-B2 AIS 55m SLE 400 ppm
(l) HadCM3L-B1 No AIS 400 ppm
(m) GISS MMCO 456 ppm
(n) CESM1 400 ppm
Salinity
38
36
34
32
30
28
26
24
22